ELSEVIER

MCN Molecular and Cellular Neuroscience

www.elsevier.com/locate/ymcne
Mol. Cell. Neurosci. 33 (2006) 170–179

Properties and expression of Kv3 channels in cerebellar Purkinje cells

Tiziana Sacco, Annarita De Luca, and Filippo Tempia*

Rita Levi Montalcini Center for Brain Repair, Department of Neuroscience, University of Torino, Corso Raffaello 30 I-10125 Torino, Italy

Received 5 June 2006; revised 21 July 2006; accepted 25 July 2006
Available online 1 September 2006

In cerebellar Purkinje cells, Kv3 potassium channels are indispensable for firing at high frequencies. In Purkinje cells from young mice (P4–P7), Kv3 currents, recorded in whole-cell in slices, activated at −30 mV, with rapid activation and deactivation kinetics, and they were partially blocked by blood depressing substance-I (BDS-I, 1 μM). At positive potentials, Kv3 currents were slowly but completely inactivating, while the recovery from inactivation was about eightfold slower, suggesting that a previous firing activity or a small change of the resting potential could in principle accumulate inactivated Kv3 channels, thereby finely tuning Kv3 current availability for subsequent action potentials. Single-cell RT-PCR analysis showed the expression by all Purkinje cells ($n=10$ for each subunit) of Kv3.1, Kv3.3 and Kv3.4 mRNA, while Kv3.2 was not expressed. These results add to the framework for interpreting the physiological function and the molecular determinants of Kv3 currents in cerebellar Purkinje cells.

Introduction

The fast spiking neuron (FSN) phenotype requires a brief action potential duration and a quick recovery of Na^+ channels from inactivation (Rudy and McBain, 2001). These two goals are attained by the exploitation of two highly specialized ion channels (Akemann and Knopfel, 2006): i) a resurgent Na^+ channel with an extremely fast recovery from inactivation, due to an unusual mechanism based on a peptide-mediated channel block, identified as the β_4 subunit (Grieco et al., 2005) but also mimicked by an exogenously applied peptide toxin (Schiavon et al., 2006); ii) K^+ channels of a subfamily (Kv3 or KCNC), which have very fast activation and deactivation kinetics associated with a high threshold for activation (Rudy and McBain, 2001). These properties of Kv3 channels cause a very fast action potential repolarization followed by a brief afterhyperpolarization, which allows a rapid recovery of Na^+ channels from inactivation. Kv3 channels assemble from subunits that in mammals are coded by four genes, named KCNC1–4 (Kv3.1–Kv3.4 subunits). Homomeric Kv3.1 and Kv3.2 channels, in heterologous expression systems, produce sustained currents, while Kv3.3 and Kv3.4 produce currents respectively with a slow and fast rate of inactivation (Rudy and McBain, 2001).

Cerebellar Purkinje cells (PCs) are FSNs, which express both a resurgent Na^+ current (Raman et al., 1997) and Kv3 K^+ channels (Martina et al., 2003; McKay and Turner, 2004). Kv3 currents have been studied in outside-out somatic and dendritic patches pulled from PCs from rats in a late phase of development, when they express the Kv3.3 and Kv3.4 subunits (Martina et al., 2003; McKay and Turner, 2004). Under these conditions, Kv3 currents were found to inactivate either with a double exponential time course (rapid time constant 10–20 ms; slow time constant 0.2–0.5 s) with no significant difference between soma and dendrites (Martina et al., 2003) or with a single, slow time constant (0.5–1 s; McKay and Turner, 2004). The latter study also described a significant voltage dependence of slow inactivation with a $V_{1/2}$ (−51.7 mV) very close to the threshold for action potentials. The time course of recovery from inactivation was not investigated, so that it is uncertain whether channel inactivation can accumulate at subthreshold voltages and affect the amount of Kv3 current available to enable fast spiking.

In this study, we show that mouse PCs, at 7 postnatal days of age, when a dendritic tree with adult branching pattern is already present, although at the beginning of its development, exhibit large Kv3 currents. Such currents show the rapid activation and deactivation properties of Kv3 channels, but they also slowly inactivate at subthreshold potentials and they even more slowly recover from inactivation. Thus, we show for the first time that these currents can accumulate inactivation and that this can occur near the resting membrane potential of Purkinje neurons.

These currents are correlated with an expression in 100% of PCs of Kv3.1, Kv3.3 and Kv3.4 mRNAs. Provided that these mRNAs are indeed translated and the proteic subunits are inserted in the plasma membrane, this result suggests that in these cells Kv3 currents might be due to heteromeric channels composed by a combination of these three subunits, although the presence of homomeric channels in separate cellular regions cannot be excluded. Our single-cell RT-PCR analysis adds new data to the discussion of a subject where contrasting results have been reported. Regarding Kv3.1, a low but detectable expression was shown by Perney et al. (1992) and Weiser et al. (1994), while a lack of

* Corresponding author. Fax: +39011 670 7708.
E-mail address: filippo.tempia@unito.it (F. Tempia).
Available online on ScienceDirect (www.sciencedirect.com).

1044-7431/$ - see front matter © 2006 Elsevier Inc. All rights reserved.
doi:10.1016/j.mcn.2006.07.006

expression was reported by Weiser et al. (1995), Martina et al. (2003) and McMahon et al. (2004). Regarding Kv3.4, Weiser et al. (1994) reported a weak expression by in-situ hybridization, while by immunohistochemistry the results depended on the type of antibody used (Veh et al., 1995; Laube et al., 1996; Martina et al., 2003).

Results

Isolation of the Kv3 component from voltage-dependent K^+ currents in PCs

In order to study Kv3 currents in cerebellar PCs, voltage-dependent/Ca^{2+} independent K^+ currents activating at high threshold potentials were isolated from other active conductances. The properties of Kv3 currents were studied in whole-cell configuration in patch-clamp recordings from PCs in cerebellar slices from young mice (4–7 postnatal days). Na^+ currents were blocked by TTX (0.5 μM), while Ca^{2+} currents and Ca^{2+} activated currents were eliminated by omitting this ion and adding EGTA in both extra- and intracellular solutions (respectively 100 μM and 10 mM EGTA). In a previous study, it was shown that PCs possess A-type voltage-dependent K^+ currents ($I_{K(A)}$) that activate at subthreshold potentials, which are insensitive to 4 mM TEA and are completely inactivated at −40 mV or more positive voltages (Sacco and Tempia, 2002). We exploited the fact that at a holding potential (V_H) of −40 mV $I_{K(A)}$ currents were not present to isolate the residual voltage-dependent/Ca^{2+} independent K^+ currents. As a first test of the presence of the highly TEA-sensitive Kv3 currents in these conditions, the dose–response curve to TEA block of such residual currents evoked by voltage steps from a V_H of −40 mV to 0 mV was measured (Figs. 1A–C). In fact, all other known K^+ channels sensitive to submillimolar concentrations of TEA were either inhibited by the absence of Ca^{2+} (BK channels) or were previously shown not to be expressed by PCs under the same experimental conditions used in this study (Kv1.1 channels; Sacco and Tempia, 2002). The currents evoked by depolarizing steps from a V_H of −40 mV to test voltages ranging from −40 to 0 mV were inhibited by TEA in a dose-dependent manner (Figs. 1A–C). TEA was applied at increasing concentrations until the effect of each dose reached a steady level (Fig. 1B). The dose–response curve obtained from 10 PCs (Fig. 1C) was well described by a single Hill function (see Eq. (1)) with an IC_{50} of 108 μM and a Hill coefficient of 0.78. This finding suggests that the residual currents evoked from a V_H of −40 mV were entirely or mainly due to channels with a very high sensitivity to TEA, as

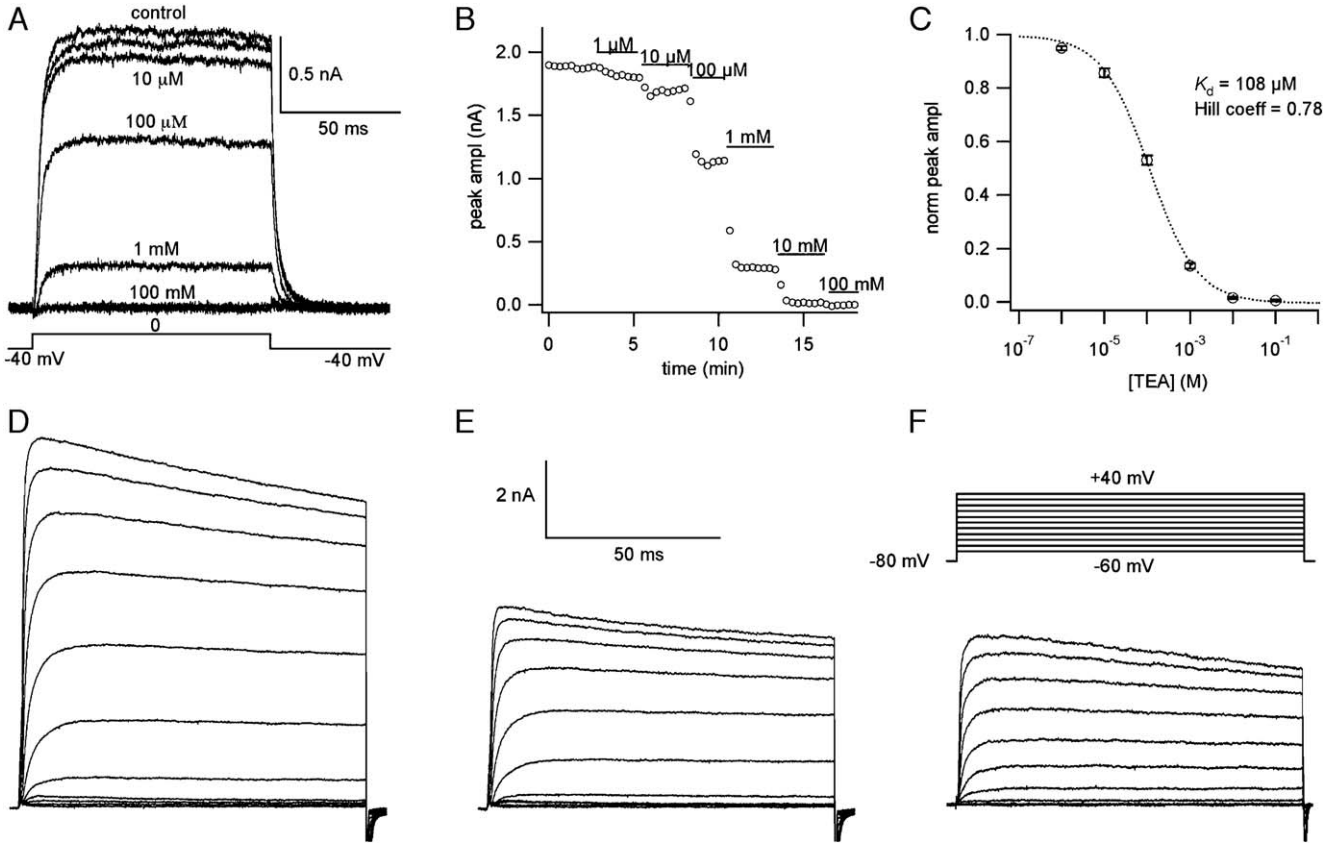

Fig. 1. TEA sensitivity of voltage-dependent/Ca^{2+} independent K^+ currents in PCs. (A) Whole-cell I_K evoked in a PC by 100 ms pulses from a V_H of −40 mV to 0 mV, before (control) and in the presence of 1 μM, 10 μM, 100 μM, 1 mM, 10 mM and 100 mM TEA. (B) Time course of the block of I_K in a PC by TEA applied at different concentrations. (C) Dose–response plot of the normalized peak amplitude as a function of TEA concentration (n = 10). Data points were fitted (dotted line) with a single Hill function (see Eq. (1)) with IC_{50} of 108 μM and Hill coefficient of 0.78. Error bars are SE. (D) Voltage-dependent Ca^{2+} independent K^+ current of one PC obtained by 100 ms steps ranging from −60 mV to +40 mV, from a V_H of −80 mV. (E) Voltage-dependent Ca^{2+} independent K^+ current recorded with the same protocol used in D but in the presence of 100 μM TEA. (F) Voltage-dependent Ca^{2+} independent K^+ currents sensitive to 100 μM TEA, obtained by the subtraction of the currents shown in panel E from the currents shown in panel D. The voltage protocol shown below the traces in panel F is valid for D–F.

described for the Kv3 subfamily, validating this protocol for the isolation of Kv3 currents. However, although no other current with a lower sensitivity to TEA was detected, we cannot exclude a minor component in the millimolar range.

The sensitivity of Kv3 currents to TEA was utilized to design an alternative procedure to isolate them from $I_{K(A)}$. In fact, even in the case of multiple components in the current studied from a V_H of −40 mV, the only currents blocked by 100 μM TEA in these conditions were certainly those due to Kv3 channels, which at this concentration were about half inhibited. Such TEA subtraction protocol allowed us to isolate Kv3 currents also from a hyperpolarized V_H. Total voltage-dependent/Ca^{2+} independent K^+ currents were evoked by steps from a V_H of −80 mV to voltages ranging from −60 to +40 mV (Fig. 1D). The addition of 100 μM TEA should affect exclusively the Kv3 component (Fig. 1E), so that the TEA-sensitive component obtained by subtraction (Fig. 1F) should be a pure Kv3 current. In order to validate this hypothesis, the voltage dependence of activation was studied independently using the two complementary protocols (Fig. 2D).

Voltage dependence and kinetics of the Kv3 current

Since Kv3 currents showed a slow decay, the steady-state inactivation was studied in Kv3 currents isolated by subtraction of

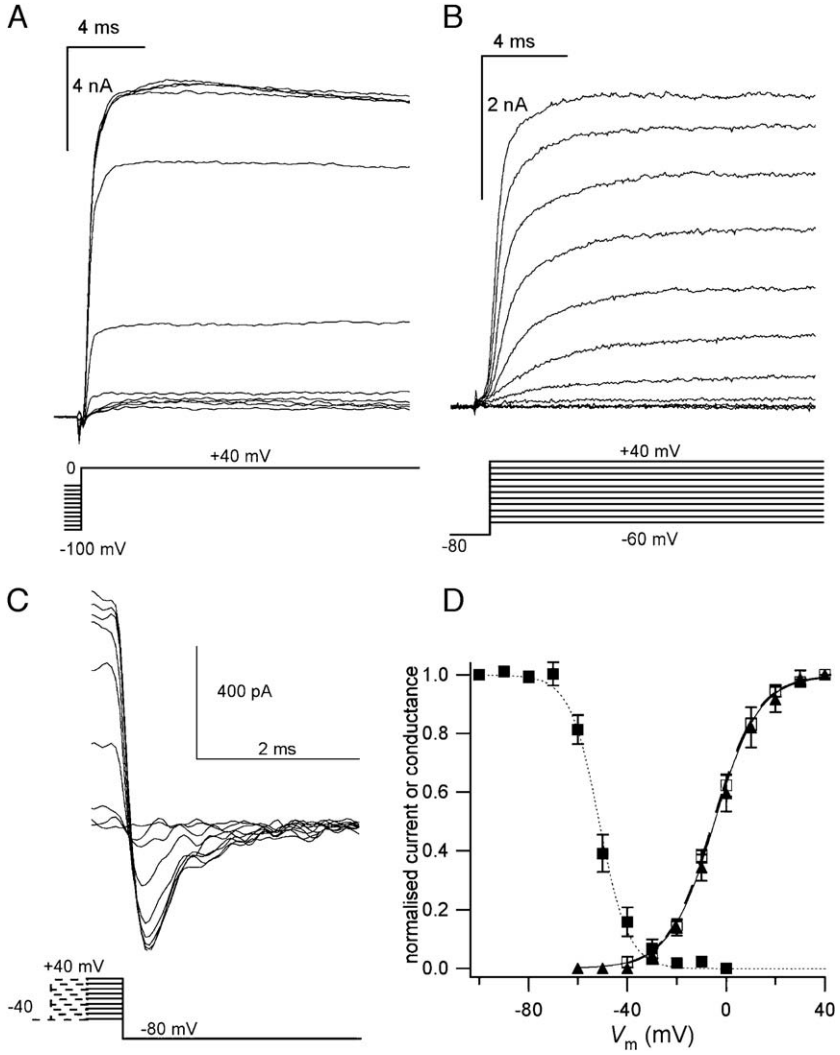

Fig. 2. Voltage dependence of the steady-state inactivation and activation of Kv3 currents. (A) Initial part of the traces of 100 μM TEA-sensitive current (Kv3 current) obtained by subtraction of voltage-dependent Ca^{2+} independent K^+ current recorded in presence of 100 μM TEA from the same current before TEA addition. Both currents were evoked by 100 ms steps to +40 mV following 30 s pre-pulses to voltages from −100 to 0 mV in 10 mV increments. The voltage protocol is shown below the traces. (B) Initial part of traces of 100 μM TEA-sensitive current obtained by subtraction as described above. The currents were evoked by pulses ranging from −60 mV to +40 mV from a V_H of −80 mV. The voltage protocol is shown below the traces. (C) Tail currents evoked by stepping back to −80 mV from 20 ms test voltages ranging from −40 mV to +40 mV, from a V_H of −40 mV. The voltage protocol is shown below the traces. (D) Filled squares: steady-state inactivation curve obtained by plotting the normalized peak amplitudes of the currents obtained by the protocol shown in panel A *versus* the pre-pulse voltage (from −100 mV to 0 mV). The dotted line is the best fitting Boltzmann function (half inactivation voltage: −51.6 mV, slope factor: 5.93 mV; $n=4$); error bars are SE; (D) open squares and filled triangles: activation curve obtained in two different ways: i) by plotting the normalized conductance relative to the currents obtained by the protocol shown in panel B (filled triangles); ii) by plotting the normalized peak amplitudes of the tail currents obtained by the protocol shown in C (open squares). The solid line and the dashed line are the best fitting Boltzmann functions of the activation curve obtained respectively with protocol i (half activation=−4.61 mV and slope factor: 9.11 mV; $n=5$) and ii (half activation=−5.72 mV and slope factor: 9.08 mV; $n=6$); error bars are SE.

the K^+ current insensitive to 100 μM TEA from the total K^+ current. Currents were evoked by a step to the test voltage of +40 mV, preceded by a pre-pulse of 30 s to potentials from −100 to 0 mV from a V_H of −80 mV. The peak amplitudes at +40 mV were normalized to the current obtained from the pre-pulse at −100 mV and plotted *versus* the pre-pulse voltages (Fig. 2D, filled squared). The peak current decreased towards positive pre-pulse potentials, following a Boltzmann function (see Eq. (2)) with a half inactivation voltage of −51.6±1.69 mV and a slope factor of 5.93±0.75 mV (n=4). To study the voltage dependence of activation, currents were obtained, in separate experiments, with both isolation protocols. With the 100 μM TEA subtraction protocol, Kv3 currents were evoked by depolarizing pulses ranging from −60 to +40 mV from a V_H of −80 mV (Fig. 2B). The conductances calculated from peak current amplitudes were normalized to the value at +40 mV and plotted *versus* the test voltage (Fig. 2D, filled triangles). This protocol allowed us to detect the threshold for activation of Kv3 currents in PCs at about −30 mV, clearly above the threshold for action potential generation. The normalized data points were fitted by a Boltzmann function (solid line) with a half activation voltage of −4.61±1.19 mV and a slope factor of 9.11±1.01 mV (n=5). The study of the voltage dependence of activation was repeated with the isolation protocol utilizing the V_H of −40 mV without any pharmacological treatment. In fact, our steady-state inactivation curve shows that at this voltage Kv3 currents are not completely inactivated, but about 20% of the channels are available (Fig. 2D). Moreover, at −40 mV, the activation is absent or negligible. The normalized conductance relative to the currents evoked from −40 mV was measured as the peak amplitude of tail currents obtained by stepping back to −80 mV from depolarizing pulses ranging from −40 to +40 mV with 20 ms of duration, at a time when the channels were open and no significant inactivation occurred (Figs. 2C–D, open squares). The normalized data points were fitted by a Boltzmann function (Fig. 2D, dashed line), with a half-maximal activation of −5.72± 1.52 mV and a slope factor of 9.08±0.97 mV (n=6). This result is superimposable to the activation curve obtained with the 100 μM TEA subtraction protocol from V_H of −80 mV.

The kinetics of activation and deactivation were studied from a V_H of −40 mV, without TEA. The activation kinetics of Kv3 currents was measured by fitting with a single exponential function (see Eq. (3)) the first part of the current evoked by pulses to voltages between −40 and +40 mV, in 10 mV increments, from a V_H of −40 mV (Fig. 3A). The decay of tail currents, which reflects channel deactivation, was studied by pulses to voltages between −80 and 0 mV following 20 ms pre-pulses to +40 mV, from a V_H of −40 (Fig. 3B, only tails are shown). Tail currents were fitted with single exponential functions (see Eq. (3)). The activation and deactivation time constants were plotted together *versus* the voltage. The data point distribution was fitted by an equation described by the Hodgkin–Huxley model (see Eq. (4)), giving a bell-shaped curve (Fig. 3C; $5 \leq n \leq 12$). The deactivation kinetics of Kv3 currents was strongly voltage-dependent: at −20 mV the deactivation time constant was 7.40±0.75 ms (n=10) while at −60 mV it was 1.35±0.21 ms (n=8). The activation kinetics of Kv3 currents was also strongly voltage-dependent: at −10 mV the activation time constant was 6.64±0.69 ms (n=11), while at +40 mV it was 0.70±0.08 ms (n=12).

The recovery from inactivation of Kv3 currents was studied with the isolation protocol based on the subtraction of the currents insensitive to 100 μM TEA from the total K^+ current. Currents were evoked by paired depolarizing pulses to +40 mV starting from a V_H of −80 mV with a variable inter-pulse interval (delta t) ranging between 0.5 and 24 s. The duration of the first pulse was set at 1 s, which, at the test potential of +40 mV, produced an almost complete inactivation. The degree of inactivation was expressed as the ratio of the peak current of the second pulse (I_2) relative to the first one (I_1). The time course of recovery from inactivation was well described by a double exponential function (dotted line, see Eq. (5); Fig. 4B) with a faster component with a time constant of 0.78±0.39 s (n=4), which accounted for 18.1%, and a slower component with a time constant of 9.16±0.87 s (n=4), which accounted for 81.8%. The decay of Kv3 currents was also studied by the subtraction protocol (Fig. 4C). Currents were evoked by 15 s depolarizing steps to 0, +20 and +40 mV, from V_H −80 mV. In order to obtain a full recovery from inactivation between steps,

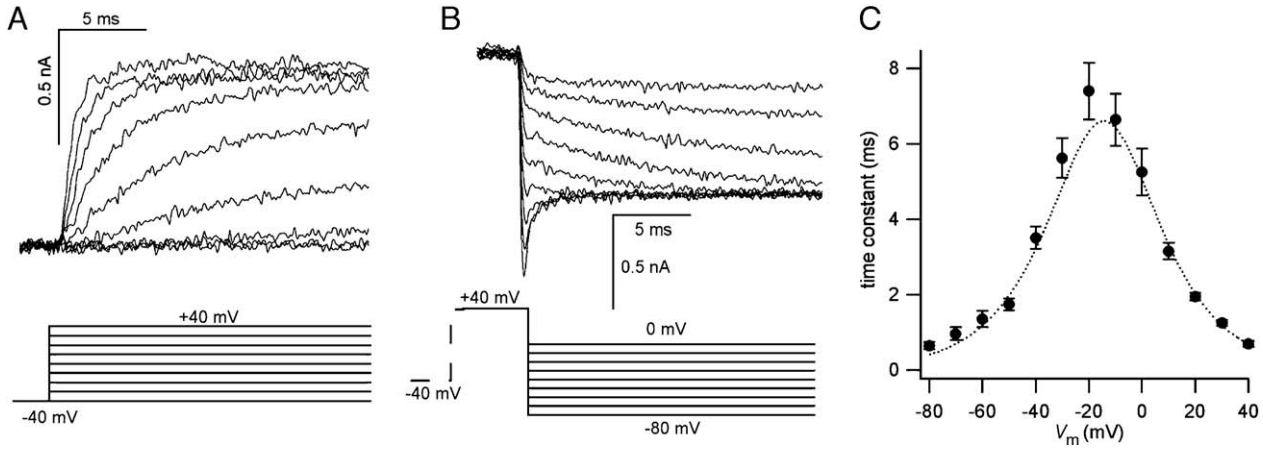

Fig. 3. Activation and deactivation kinetics of Kv3 currents. (A) Initial part of the currents evoked by 20 ms pulses to voltages between −40 mV and +40 mV, in 10 mV increments from a V_H of −40 mV. (B) Tail currents evoked by 20 ms pulses to voltages between −80 mV and 0 mV in 10 mV increments following pre-pulses of 20 ms duration to +40 mV, from a V_H of −40 mV. In panels A and B the voltage protocols are shown below the traces. (C) Deactivation time constants of tail currents (from −80 to −10 mV) and activation time constants (from −10 to +40 mV) measured by single exponential fittings ($5 \leq n \leq 12$). The dotted line is the best fitting curve of the kinetics function of the Hodgkin–Huxley model (see Eq. (4)); bars are SE.

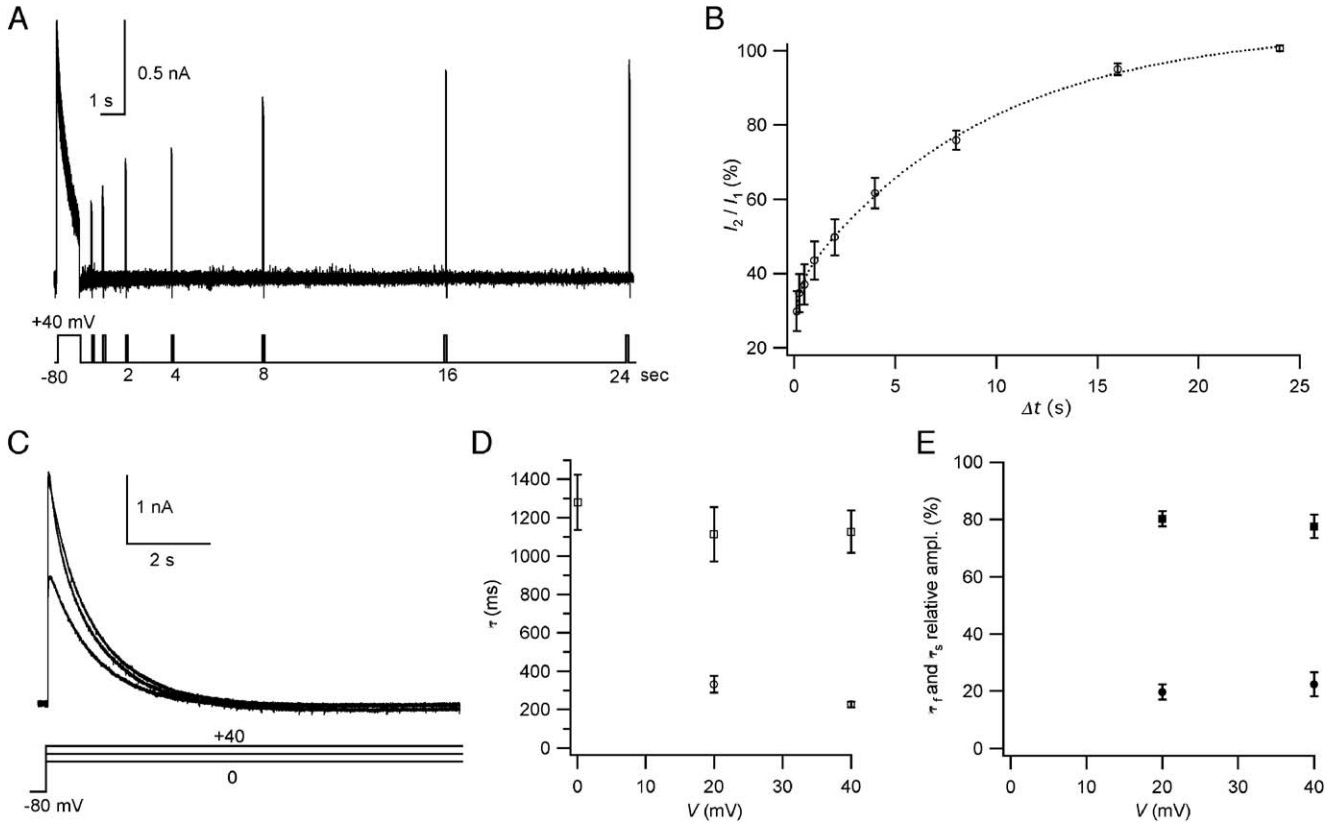

Fig. 4. Inactivation and recovery from inactivation of Kv3 currents. (A) 100 μM TEA-sensitive currents obtained by subtraction of voltage-dependent Ca^{2+} independent K^+ currents recorded in the presence of 100 μM TEA from the same currents before TEA application. Currents were evoked by paired pulses to +40 mV, from a V_H of −80 mV: first pulse (I_1), 1 s of duration; second pulse (I_2), 100 ms of duration, at a variable inter-pulse interval (delta t) ranging between 0.5 and 24 s. The voltage protocol is shown below the traces. (B) Time course of recovery from inactivation; the ratio of the peak amplitudes of the second current (I_2) over the first current (I_1) is plotted as a function of the inter-pulse interval. The time course of recovery was fitted (dotted line) by a double exponential function (see Eq. (5)) with a fast time constant of 0.78 s (18.1%) and a slow time constant of 9.16 s (81.8%). (C) 100 μM TEA-sensitive current evoked by 15 s voltage steps (60 s interval) to 0 mV, +20 mV and +40 mV from a V_H of −80 mV. (D) Voltage dependence plot of the time constants of the currents evoked by the protocol shown in panel C. Fast (circles) and slow (squares) time constants obtained by the single (0 mV) or double (+20 and +40 mV) exponential fittings (n=5). (E) Relative amplitude (%) of the fast (circles) and slow (squares) time constants plotted as a function of voltage (n=5); error bars are SE.

before each depolarization, the cell was kept for 30 s at the V_H of −80 mV. At 0, +20 and +40 mV, Kv3 currents had a pronounced time-dependent inactivation, which in about 6 s reached a constant level (Fig. 4C). At +20 and +40 mV, the time course of inactivation (Fig. 4D) was well described by a double exponential function (see Eq. (5)), while at 0 mV it followed a single exponential function (see Eq. (3)). The single time constant at 0 mV was 1279.7±144.9 ms (n=5) that was very similar to the slow time constants at +20: 1113.9±140.3 ms (n=5) and at +40 mV: 1126.9±109.6 ms (n=5). The fast time constant at +20 mV was 331.7±43.8 ms (n=5) and at +40 mV was 227.3±14.9 ms (n=5). The relative contribution of the fast and slow exponentials was measured by extrapolating the function to 1 ms after the beginning of the voltage step. The slower time constant accounted for 80.2±2.6% at +20 mV (n=5) and for 77.5±4.2% at +40 mV (n=5) (Fig. 4E).

Effect of BDS-I toxin on PC Kv3 currents

We have tested the effect of BDS-I (~1 μM) on Kv3 currents of cerebellar PCs. Kv3 currents were isolated, as above, by subtraction of 100 μM TEA insensitive current from the total K^+ currents. The currents were evoked by 500 ms pulses to +20 mV from a V_H of −80 mV (Fig. 5A). BDS-I (~1 μM) caused a reduction of Kv3 currents of 24.3%±1.9% (Fig. 5B; n=5). Such sensitivity to BDS-I is in line with the Kv3 identity of these currents.

Expression of Kv3 channels in cerebellar PC at 7 postnatal days

In parallel with the characterization of the biophysical properties of Kv3 currents in PCs, we have studied in these cells the expression of the four known Kv3 genes with the single-cell RT-PCR technique. We tested the expression of Kv3.1 (n=10), Kv3.2 (n=10), Kv3.3 (n=10) and Kv3.4 (n=10) transcripts in mouse PCs using mouse specific primers (see methods). PCs were harvested in slice preparations, in which they were promptly identified for the large size, the distinctive morphology and the localization in the PC layer. Harvesting of other material, especially of granule cells, was carefully avoided to ensure the specificity of the detection. In order to confirm the identity of harvested PCs and to have a positive control in case of lack of expression of the Kv3 subunit, all single-cell RT-PCR reactions were run as duplex with primers for one Kv3 subunit and for calbindin, which in 7-day-old cerebellum is known to be expressed selectively by all PCs. All the PCs analyzed showed expression of Kv3.1, Kv3.3 and Kv3.4 channels

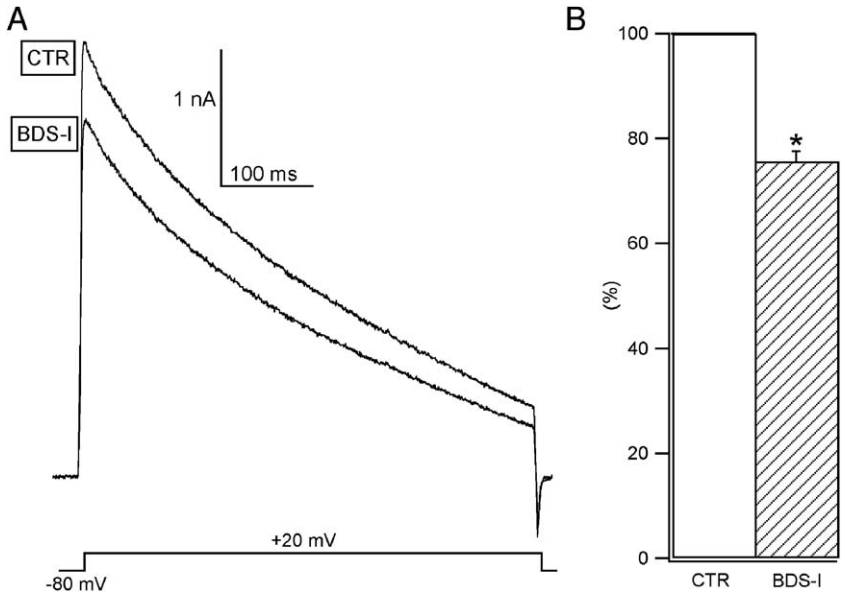

Fig. 5. Effects of BDS-I on Kv3 currents. (A) Kv3 currents obtained by subtraction of the voltage-dependent Ca^{2+} independent K^+ current recorded in presence of 100 μM TEA from the same current before TEA addition. Both currents were evoked by a 500 ms pulse to +20 mV from a V_H of −80 mV. CTR: control trace; BDS-I: after BDS-I application. The voltage protocol is shown below the traces. (B) Mean of the percentage of the peak amplitude of the current, in the control (empty column) and during BDS-I block (hatched column); $n=5$; error bar is SE. Asterisk shows statistically significant difference ($P<0.05$).

(Fig. 6), whereas Kv3.2 expression was completely absent despite positive controls, including calbindin, giving the expected products.

Discussion

The firing properties of neurons strictly depend on the type and amount of ion channels present in the plasma membrane. FSNs, including PCs, require channels with special functional features, such as Kv3 voltage-dependent K^+ channels (Rudy and McBain, 2001; Akemann and Knopfel, 2006). In agreement with previous studies (Sacco and Tempia, 2002; Martina et al., 2003; McKay and Turner, 2004), we show that PCs express very large voltage-dependent and Ca^{2+} independent K^+ currents sensitive to sub-millimolar doses of TEA. In our study, in order to isolate such currents, we used two independent experimental protocols, which were both effective, as shown by the superimposable results obtained for the voltage dependence of activation. The properties of the currents and their monotonic inhibition by extracellular TEA suggest that the currents were due to a single class of channels, corresponding to the Kv3 subfamily of voltage-dependent K^+ channels. The single-cell RT-PCR analysis of the expression of the four Kv3 genes indicates a homogeneous expression by PCs at P7 of Kv3.1, Kv3.3 and Kv3.4. This result is in line with the absence of significant differences of Kv3 current properties between PCs.

The activation threshold at about −30 mV is more negative than that shown for Kv3 channels expressed in heterologous systems (Rudy and McBain, 2001), but it is consistent with other FSNs (Baranauskas et al., 2003). The kinetics of activation and deactivation are in agreement with previous studies (Martina et al., 2003; McKay and Turner, 2004). A property peculiar of Kv3 currents of PCs is the presence of a significant degree of inactivation, which has been studied in detail for the first time in this report. Martina et al. (2003) have shown that, in outside-out patches, either from PC soma or from dendrites, Kv3 currents inactivate with a double exponential time course, with a faster time constant of 10–20 ms and a slower one of 0.2–0.5 s. The lack, in our study and in the report by McKay and Turner (2004), of a very fast component of decay of 10–20 ms is very unlikely due to voltage-clamp problems since our currents show well resolved kinetics of activation and deactivation with time constants shorter than 1 ms. A more likely explanation is the fact that, in the experiments by Martina et al. (2003), no protocol was used to isolate Kv3 currents from other voltage-dependent K^+ conductances. Actually, in their recordings, both TEA and 4-aminopyridine dose–response curves displayed a residual component of about 20% which can be attributed to other channel subfamilies (Martina et al., 2003). The co-existence of Kv3 with other K^+ currents might explain the fast time constant, which is in line neither with our results nor with those of McKay and Turner (2004). Another possible explanation for the presence of such fast component of decay is the outside-out preparation, which could alter the intracellular modulation mechanisms more than whole-cell recording.

We show that, at positive potentials, Kv3 currents of PCs follow a double exponential decay, in which the main time constant (accounting for about 80% of the decay) is slightly longer than 1 s (1.1–1.3 s). The secondary, fast time constant was 0.2–0.3 s, in the range of the decay of outside-out patches from older PCs (Martina et al., 2003). The time constant of 0.5–1 s described by McKay and Turner (2004) seems intermediate between our values. Our results validate the study by McKay and Turner (2004), in which K^+ currents were recorded with an extracellular solution containing a cocktail of K^+ channel blockers in order to isolate the Kv3 component. In addition to such pharmacological isolation, these authors also used a TEA subtraction protocol similar to ours, but with a higher concentration (1 mM). We chose to apply TEA at 100 μM because the aim of this protocol was not to describe the overall amplitude of Kv3 currents, which were recorded with a non-physiological intracellular K^+ concentration, but to study the

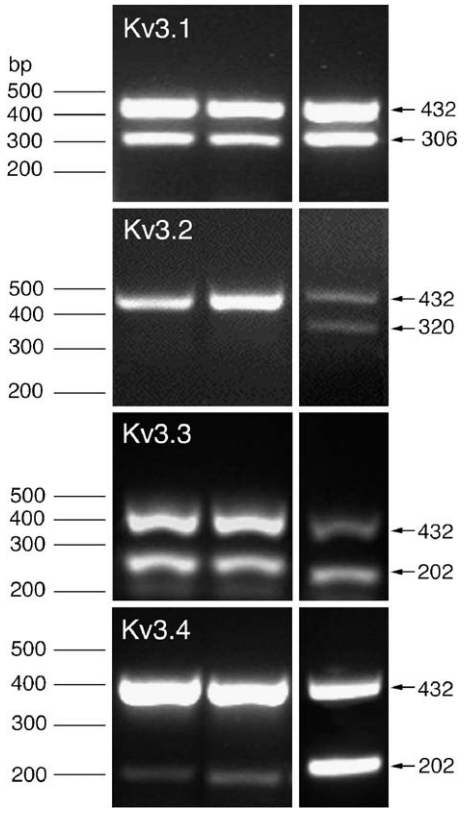

Fig. 6. Single-cell RT-PCR of the genes of Kv3 subunits in PCs at 7 postnatal days. RT-PCR products from single PCs for each Kv3 subunit in duplex with calbindin (left pairs of lanes). Right lanes are positive controls (total mouse P7 cerebellum). The molecular weights used are 100 bp markers (horizontal lines on the left). In the negative control (not shown), the amplification was performed without template. The arrows on the right indicate the amplicons of each subunit (Kv3.1, 306 bp, Kv3.2, 320 bp; Kv3.3, 202 bp; Kv3.4, 202 bp) and of calbindin (432 bp).

biophysical properties of Kv3 currents without any other contaminating component. The fact that our TEA subtraction protocol did not recover the whole extent of Kv3 currents did not affect their functional properties, as demonstrated by the superimposable data obtained with the other isolation protocol, based on the V_H of −40 mV.

Most of the recovery from inactivation (about 80%) occurs with a very long time constant of about 9 s. This finding has important physiological consequences, such as the possibility of accumulation of inactivated channels during repetitive action potential firing, which in PCs in vivo is very common (Savio and Tempia, 1985). This finding, together with the presence of steady-state inactivation at potentials below action potential threshold, can potentially cause a different channel availability depending on the recent history of the cell membrane potential. As a consequence, subsequent action potentials, which in Purkinje cells reach a peak in the voltage range of full Kv3 current activation (+20 mV or more, Fig. 2D), instead of completely exploiting all Kv3 channels present in the plasma membrane, would have a reduced pool of Kv3 channels available. For example, at −60 mV there are about 20% less channels available than at −70 mV (see Fig. 2D). Therefore, a hyperpolarization lasting several seconds, causing recovery from inactivation of a relevant fraction of Kv3 channels, is likely to cause an increase of the Kv3 current evoked by the initial action potentials of a sudden burst of activity. In contrast, short changes in membrane potential, lasting less than 1 s, would produce only minimal changes in the fraction of available Kv3 channels since only a minor component of the recovery from inactivation occurs with a faster time constant shorter than 1 s (0.5–1 s). This hypothesis requires experimental evidence from future experiments.

The sensitivity to BDS-I is in accordance with the Kv3 identity of at least part of the currents. While a former report suggested a selectivity of this toxin for the Kv3.4 subunit (Diochot et al., 1998), a more recent study showed that also Kv3.1 and Kv3.2 display a similar sensitivity to BDS-I, while Kv3.3 was not studied (Yeung et al., 2005). Therefore, our finding of the blocking effect of this toxin does not allow us to further distinguish between the Kv3 subunits responsible for the current, but only to strengthen its ascription to Kv3 channels. The fact that the block was only partial (about 24%) can be attributed to an incomplete penetration of BDS-I inside the tissue of the slice or to a lower sensitivity of Kv3 channels in PCs relative to previous studies on cultured or dissociated cells (Diochot et al., 1998; Ono et al., 2005; Yeung et al., 2005). Alternatively, it is also possible that a component of the current is sensitive to BDS-I while another component is insensitive.

The expression in all PCs analyzed of Kv3.1, Kv3.3 and Kv3.4 subunits suggests that, at postnatal day 7, Kv3 channels in these neurons might be composed by these three types of subunits. However, it is also possible that one or two of these mRNAs is not translated or that the protein is not inserted in the plasma membrane or that homomeric channels might be assembled in separate cellular regions. This result is in agreement with previous studies that reported the expression, in PCs of adult rats, of Kv3.1, Kv3.3 and Kv3.4 (Perney et al., 1992; Weiser et al., 1994), while it contrasts with other reports (Weiser et al., 1995; Martina et al., 2003; McMahon et al., 2004), which failed to detect Kv3.1 expression in this cell type. A possible explanation is that the RNA detection techniques used by Perney et al. (1992), by Weiser et al. (1994) and also in the present study are more sensitive than the immunohistochemical detection of the protein utilized by the other studies (Weiser et al., 1995; Martina et al., 2003; McMahon et al., 2004). Alternatively, this discrepancy might be explained if the Kv3.1 gene is transcribed in PCs, while the protein is present in these cells at low or negligible levels because of posttranscriptional silencing or very fast protein degradation of the Kv3.1 subunit.

In spite of the more intense labeling of distal dendrites with an antibody against the Kv3.4 subunit (Martina et al., 2003), the possibility that this cellular compartment contains homomeric Kv3.4 channels is unlikely because our recordings do not show a fast component attributable to this subunit. Furthermore, outside-out patches pulled from PC somata or dendrites showed similar kinetic properties, suggesting a similar subunit composition (Martina et al., 2003). Our results extend this notion to the most distal compartments of dendrites, which were not investigated in outside-out patches.

Our results suggest that, in PCs, Kv3 currents might be due to channels with a complex subunit composition. Our results indicate for the first time that such currents, which in PCs are the main determinant of action potential repolarization and of the fast afterhyperpolarization (McKay and Turner, 2004), do not have a fixed intensity, but the resting membrane potential can finely tune the amount of available Kv3 channels because a fraction of them is inactivated even at subthreshold potentials. Additional mechanisms, which could be involved in the

modulation of Kv3 currents, are phosphorylation, the presence of accessory subunits or the ratio of expression of spice variants (Rudy and McBain, 2001).

The fact that Kv3 channels play an important role in cerebellar physiology is indicated by a recent finding that one form of human cerebellar ataxia is linked to mutations in the KCNC3 gene (Waters et al., 2006), coding for the Kv3.3 subunit, which is the most abundantly expressed Kv3 subunit in PCs (Weiser et al., 1994). In addition, also Kv3.1/Kv3.3 double knockout mice are severely ataxic and have a marked broadening of action potentials in cerebellar granule cells and PCs (Espinosa et al., 2001; Matsukawa et al., 2003). Kv3.3 single mutant mice are not overtly ataxic, but they have a 100% increase of PC action potential duration and lack harmaline-induced tremor, indicating a disrupted function of the olivo-cerebellar circuit (McMahon et al., 2004). Our results, showing that PCs express the transcripts of 3 subunits of the Kv3 family, add to the framework for interpreting the mechanisms underlying these deficits. The picture is further enriched by the possibility of fine tuning of Kv3 currents by subtle changes of the resting membrane potential.

Experimental methods

Slice preparation and patch-clamp recording

Voltage-clamp recording experiments were performed using the whole-cell configuration of the patch-clamp technique at room temperature (22–25°C) on CD-1 mice of either sex, 4–7 days old (P4–P7). Cerebellar slices were obtained following a previously described technique (Llinas and Sugimori, 1980; Edwards et al., 1989). Briefly, the animals were anesthetized with isoflurane (Isoflurane-Vet, Merial, Italy) and decapitated. The experiments were approved by the University Bioethical Committee of the University of Torino. The cerebellar vermis was removed and transferred to an ice-cold extracellular saline solution containing (in mM); 125 NaCl, 2.5 KCl, 2 $CaCl_2$, 1 $MgCl_2$, 1.25 NaH_2PO_4, 26 $NaHCO_3$, 20 glucose, which was bubbled with 95% O_2/5% CO_2 (pH 7.4). Parasagittal cerebellar slices (200 μm thickness) were obtained using a vibratome (Vibroslice 752, Campden Instruments Ltd, UK) and kept for 1 h at 35°C before transferring them to the experimental setup. A single slice at a time was placed in the recording chamber and continuously perfused at room temperature (22–25°C) with the saline solution bubbled with the 95% O_2/5% CO_2. A Purkinje cell was visualized using a 40× water-immersion objective of an upright microscope (E600FN, Eclipse, Nikon, Japan), and its upper surface was cleaned by a glass pipette, pulled from sodalime glass to a tip diameter of 10–15 μm, containing the saline solution (Edwards et al., 1989). Pipettes of borosilicate glass, with a tip diameter of 2–3 μm, with resistances between 2.5 and 3.0 MΩ were used for patch-clamp recording. The internal solution had the following composition (in mM): 25 KCl, 148 NMDG, 4 $MgCl_2$, 10 HEPES, 4 Na_2ATP, 0.4 Na_3GTP, 10 EGTA and the pH was adjusted to 7.3 with HCl and filtered at 0.2 μm. The liquid junction potential with the extracellular saline solution was 1.5 mV. Absolute membrane voltages reported in the text are not corrected for such liquid junction potential. All recordings were performed from the soma of PCs, at room temperature (22–25°C) in voltage-clamp mode, in whole-cell configuration, using an EPC-9 patch-clamp amplifier (HEKA Elektronik, Lambrecht/Pfalz, Germany). Recordings were accepted only if the series resistance was less than 8.0 MΩ (range: 5.0–8.0 MΩ), and the series resistance compensation was set at 90%. Data were filtered and digitized using the built-in filter and analog to digital interface of the EPC-9 amplifier. Recordings were filtered at 8.6 kHz and digitized at 20 kHz, except for the study of the time course of inactivation (filter 0.5 kHz; sampling rate 1 kHz). Digitized data were stored on a Macintosh computer (G3, Apple computer, Cupertino, CA, USA) using the Pulse software (HEKA Elektronik, Lambrecht/Pfalz, Germany). Capacitive transients were subtracted using a P/5 protocol for the recordings from a holding potential (V_H) of −40 mV, while for the other recordings capacitive transients were not subtracted because they were eliminated by the subtraction of the traces in TEA from the total K^+ currents. The extracellular saline solution used during recordings was prepared omitting $CaCl_2$ but it contained 5 mM $MgCl_2$, 100 μM EGTA, 0.5 mM CsCl, 0.5 μM tetrodotoxin citrate (TTX), 20 μM bicuculline. In some experiments, tetraethylammonium chloride (TEA) was also added to the extracellular solution. In extracellular solutions with high TEA concentration, osmolarity was maintained by reducing the concentration of NaCl. Drugs were applied to the slice by changing the perfusion line, except for BDS-I, which was applied directly into the recording chamber, in a solution containing 0.1% of bovine serum albumin (BSA), via a 1 ml syringe. BDS-I application was preceded by at least 2 min of slice perfusion with BSA-containing extracellular saline (0.1%). In this case, BDS-I concentration was calculated by measuring the final volume of the solution in the recording chamber after the addition of the BDS-I solution (4 μM). During incubation with BDS-I, the perfusion line was stopped for not more than 3 min. Simply stopping the perfusion for the same time had no effect on the recorded currents. All drugs were purchased from Sigma Chemical (St. Louis, MO, USA) except TTX, bicuculline, (Tocris Cookson, Langford, UK) and BDS-I (Alomone Labs, Jerusalem, Israel).

Current analysis

Data were analyzed by the commercial program Igor Pro (Wavemetrics, Lake Oswego, OR, USA). Best fitting curves were obtained by IgorPro built in functions, with the methods of χ^2 minimization. The dose–response curves for the effect of the blockers have been fitted by a single Hill equation:

$$I = \{(I_{max} - I_{min})/[1 + (x/x_0)^p]\} + I_{min} \quad (1)$$

where I_{max} and I_{min} are respectively the maximal and minimal current amplitudes, x_0 is the IC_{50}, x is the concentration of the blocker, p is the Hill coefficient.

The activation curve for test currents evoked from V_H of −40 mV was determined by normalizing the peak of tail currents at −80 mV, plotted against the test potential. For currents obtained with the TEA subtraction protocol, the activation curve was obtained by plotting the normalized conductance, calculated by dividing the peak current by the difference between the test potential and the equilibrium potential for K^+ (−59 mV in our recording conditions), against the test voltage. The voltage dependence of steady-state inactivation was obtained by normalizing the peak currents at +40 mV to the value evoked from the pre-pulse at −100 mV. The activation and inactivation data were fit with the Boltzmann equation:

$$I_{(v)} = (I_2 - I_1)/\{1 + \exp[-(V - V_{0.5})/k)]\} + I_1 \quad (2)$$

where $I_{(V)}$ is the peak current or peak conductance as a function of V_H or of the test potential, I_1 and I_2 are the peak amplitudes or conductances of the currents at respectively the most negative and most positive potentials tested, V is the holding voltage or the test potential, $V_{0.5}$ is the voltage at which the current or the conductance is half of the maximal amplitude and k represents the slope factor.

The time course of activation and deactivation of the current was obtained by fitting the data with a mono-exponential equation:

$$I_{(t)} = I_1[1 - \exp(-t/\tau)] \quad (3)$$

where $I_{(t)}$ is the current at time t, I_1 is the initial amplitude and τ is the time constant.

The voltage dependence of the deactivation and activation time constants was fitted by a bell-shaped curve derived from an equation of the Hodgkin–Huxley model:

$$f_{(v)} = 1/(\alpha + \beta) \quad (4)$$

where the activation rate coefficient $\alpha = a_0 \exp(a_k V)$ and the deactivation rate coefficient $\beta = b_0 \exp(-b_k V)$.

The decay of the current and the recovery from inactivation were obtained by fitting the data with a double-exponential equation:

$$I_{(t)} = \{I_s[\exp(-t/\tau_s)]\} + \{I_f[\exp(-t/\tau_f)]\} \quad (5)$$

where $I_{(t)}$ is the current at time t, I_s and I_f are the initial amplitudes of the two components related to τ_s and τ_f which are respectively the slow and the fast time constants.

Results throughout the manuscript are expressed as means± SEM.

Single-cell RT-PCR

eTo maximize RNA yields, cells were aspirated into a cleaning pipette by applying negative pressure. The glass capillary used had been heated at 180°C for 8 h. The capillary tips were filled with ~1 μl of sterile extracellular saline solution. Then, each cell was aspirated separately into the capillary tip and the electrode tips were broken into a 0.2 ml Eppendorf tube containing 3 μl of diethylpyrocarbonate-treated (DEPC) water. The entire RNA of each cell was retrotranscribed (RT) in a total volume of 20 μl by adding 250 ng of random primers (50 ng/μl), 0.5 mM of dNTPs, 10× RT buffer, 5 mM $MgCl_2$, 10 mM DTT, 1 μl of RNaseOUT recombinant ribonuclease inhibitor and 50 units of SuperScript II reverse transcriptase. cDNA synthesis was carried out for 50 min at 42°C and stopped by heating the mixture to 70°C for 15 min. After quenching the reaction in ice, the RNA strand in the RNA–DNA hybrid was removed by 2 units of *E. coli* RNase H for 20 min at 37°C. All reagents for the RT procedure were included in the Superscript First-Strand Synthesis System kit (Invitrogen Carlsbad, CA, USA). The single-cell cDNA was amplified by polymerase chain reaction (PCR) to detect the expression of calbindin, Kv3.1, Kv3.2, Kv3.3 and Kv3.4. The PCR for calbindin was performed to assure that analyzed cells were Purkinje cells. The whole cDNA of single-cells was used as a template for the reaction containing 0.5 mM of each primer, 2.5 mM $MgCl_2$, 0.5 mM dNTPs, 2.5 units Taq Promega DNA polymerase and buffer 10×. The primer sequences used have been modified from Xu et al. (1999) to match the mouse sequences: for Kv3.1 (NM_008421): 5′-CGTGCCGACGAGTTCTTCT-3′ and 5′-GGTCATCTCCAGCTCGTCCT-3′; for Kv3.2 (XM_193580): 5′-GGGCAAGATCGAGAGCAAC-3′ and 5′-GGTGGCGATCGAAGAAGA-3′; for Kv3.3 (NM_008422): 5′-GGCGACA GCGGTAAGATCGTG-3′ and 5′-GGTAGTAGTTGAGCACGTAGGCGA-3′; for Kv3.4 (NM_145922): 5′-CGACGATGAGCGGGAGTTGG-3′ and 5′-CAGGCAGAAGGTGGTAATGG AG-3′; for calbindin (NM_009788) 5′-AGGCGCGAAAGAAGGCTGGAT-3′ and 5′-TCCCACA CATTTTGATTCCCTG-3′. The cycling conditions were 95°C for 2 min followed by 35 cycles of 95°C for 30 s, 63°C for 30 s and 72°C for 1 min and then 2 min at 72°C for final elongation. Positive (cDNA obtained from mouse cerebellum total RNA) and negative (water instead of template) controls were amplified in the same conditions. The PCR product was run on 1.2% agarose gel stained with Gel Star (Cambrex Corporation, East Rutherford, NJ, USA) in the presence of a 100 bp DNA ladder as the molecular weight marker (Promega, Madison, WI, USA).

Acknowledgments

This work was supported by grants from MIUR (PRIN 2001 and 2003), from the University of Torino and Regione Piemonte (Ricerca Sanitaria Finalizzata, bando 2004). The technical assistance of Mrs. Luisella Milano and Dr. Federica Premoselli is acknowledged.

References

Akemann, W., Knopfel, T., 2006. Interaction of Kv3 potassium channels and resurgent sodium current influences the rate of spontaneous firing of Purkinje neurons. J. Neurosci. 26, 4602–4612.

Baranauskas, G., Tkatch, T., Nagata, K., Yeh, J.Z., Surmeier, D.J., 2003. Kv3.4 subunits enhance the repolarizing efficiency of Kv3.1 channels in fast-spiking neurons. Nat. Neurosci. 6, 258–266.

Diochot, S., Schweitz, H., Beress, L., Lazdunski, M., 1998. Sea anemone peptides with a specific blocking activity against the fast inactivating potassium channel Kv3.4. J. Biol. Chem. 273, 6744–6749.

Edwards, F.A., Konnerth, A., Sakmann, B., Takahashi, T., 1989. A thin slice preparation for patch clamp recordings from neurones of the mammalian central nervous system. Pflugers Arch. 414, 600–612.

Espinosa, F., McMahon, A., Chan, E., Wang, S., Ho, C.S., Heintz, N., Joho, R.H., 2001. Alcohol hypersensitivity, increased locomotion, and spontaneous myoclonus in mice lacking the potassium channels Kv3.1 and Kv3.3. J. Neurosci. 21, 6657–6665.

Grieco, T.M., Malhotra, J.D., Chen, C., Isom, L.L., Raman, I.M., 2005. Open-channel block by the cytoplasmic tail of sodium channel β4 as a mechanism for resurgent sodium current. Neuron 45, 233–244.

Laube, G., Roper, J., Pitt, J.C., Sewing, S., Kistner, U., Garner, C.C., Pongs, O., Veh, R.W., 1996. Ultrastructural localization of Shaker-related potassium channel subunits and synapse-associated protein 90 to septate-like junctions in rat cerebellar Pinceaux. Brain Res. Mol. Brain Res. 42, 51–61.

Llinas, R., Sugimori, M., 1980. Electrophysiological properties of in vitro Purkinje cell somata in mammalian cerebellar slices. J. Physiol. (London) 305, 171–195.

Martina, M., Yao, G.L., Bean, B.P., 2003. Properties and functional role of voltage-dependent potassium channels in dendrites of rat cerebellar Purkinje neurons. J. Neurosci. 23, 5698–5707.

Matsukawa, H., Wolf, A.M., Matsushita, S., Joho, R.H., Knopfel, T., 2003. Free full text motor dysfunction and altered synaptic transmission at the parallel fiber–Purkinje cell synapse in mice lacking potassium channels Kv3.1 and Kv3.3. J. Neurosci. 23, 7677–7684.

McKay, B.E., Turner, R.W., 2004. Kv3 K^+ channels enable burst output in rat cerebellar Purkinje cells. Eur. J. Neurosci. 20, 729–739.

McMahon, A., Fowler, S.C., Perney, T.M., Akemann, W., Knopfel, T., Joho, R.H., 2004. Allele-dependent changes of olivocerebellar circuit properties in the absence of the voltage-gated potassium channels Kv3.1 and Kv3.3. Eur. J. Neurosci. 19, 3317–3327.

Ono, K., Toyono, T., Honda, E., Inenaga, K., 2005. Transient outward K^+ currents in rat dissociated subfornical organ neurones and angiotensin II effects. J. Physiol. (London) 568, 979–991.

Perney, T.M., Marshall, J., Martin, K.A., Hockfield, S., Kaczmarek, L.K., 1992. Expression of the mRNAs for the Kv3.1 potassium channel gene in the adult and developing rat brain. J. Neurophysiol. 68, 756–766.

Raman, I.M., Sprunger, L.K., Meisler, M.H., Bean, B.P., 1997. Altered subthreshold sodium currents and disrupted firing patterns in Purkinje neurons of Scn8a mutant mice. Neuron 19, 881–891.

Rudy, B., McBain, C.J., 2001. Kv3 channels: voltage-gated K^+ channels designed for high-frequency repetitive firing. Trends Neurosci. 24, 517–526.

Sacco, T., Tempia, F., 2002. A-type potassium currents active at subthreshold potentials in mouse cerebellar Purkinje cells. J. Physiol. (London) 543, 505–520.

Savio, T., Tempia, F., 1985. On the Purkinje cell activity increase induced by suppression of inferior olive activity. Exp. Brain Res. 57, 456–563.

Schiavon, E., Sacco, T., Restano Cassulini, R., Gurrola, G., Tempia, F., Possani, L.D., Wanke, E., 2006. Resurgent current and voltage sensor-trapping enhanced activation by a β-scorpion toxin solely in Nav1.6 channel: significance in mice Purkinje neurons. J. Biol. Chem. 281, 20326–20337.

Veh, R.W., Lichtinghagen, R., Sewing, S., Wunder, F., Grumbach, I.M., Pongs, O., 1995. Immunohistochemical localization of five members of the Kv1 channel subunits: contrasting subcellular locations and neuron-specific co-localizations in rat brain. Eur. J. Neurosci. 7, 2189–2205.

Waters, M.F., Minassian, N.A., Stevanin, G., Figueroa, K.P., Bannister, J.P., Nolte, D., Mock, A.F., Evidente, V.G., Fee, D.B., Muller, U., Durr, A.,

Brice, A., Papazian, D.M., Pulst, S.M., 2006. Mutations in voltage-gated potassium channel KCNC3 cause degenerative and developmental central nervous system phenotypes. Nat. Genet. 38, 447–451.

Weiser, M., Vega-Saenz de Miera, E., Kentros, C., Moreno, H., Franzen, L., Hillman, D., Baker, H., Rudy, B., 1994. Differential expression of Shaw-related K^+ channels in the rat central nervous system. J. Neurosci. 14, 949–972.

Weiser, M., Bueno, E., Sekirnjak, C., Martone, M.E., Baker, H., Hillman, D., Chen, S., Thornhill, W., Ellisman, M., Rudy, B., 1995. The potassium channel subunit KV3.1b is localized to somatic and axonal membranes of specific populations of CNS neurons. J. Neurosci. 15, 4298–4314.

Xu, C., Lu, Y., Tang, G., Wang, R., 1999. Expression of voltage-dependent K^+ channel genes in mesenteric artery smooth muscle cells. Am. J. Physiol. 277, G1055–G1063.

Yeung, S.Y., Thompson, D., Wang, Z., Fedida, D., Robertson, B., 2005. Modulation of Kv3 subfamily potassium currents by the sea anemone toxin BDS: significance for CNS and biophysical studies. J. Neurosci. 25, 8735–8745.